Journal of Coordination Chemistry

ISSN: 0095-8972 (Print) 1029-0389 (Online) Journal homepage: http://www.tandfonline.com/loi/gcoo20

Synthesis of monosodium salts of N-(5-nitro-salicylidene)-D-amino acid Schiff bases and their iron(III) complexes: spectral and physical characterizations, antioxidant activities

Özlem Özdemir (nee Güngör), Perihan Gürkan, Musa Sarı & Tuncay Tunç

To cite this article: Özlem Özdemir (nee Güngör), Perihan Gürkan, Musa Sarı & Tuncay Tunç (2015) Synthesis of monosodium salts of N-(5-nitro-salicylidene)-D-amino acid Schiff bases and their iron(III) complexes: spectral and physical characterizations, antioxidant activities, Journal of Coordination Chemistry, 68:14, 2565-2585, DOI: 10.1080/00958972.2015.1043908

To link to this article: http://dx.doi.org/10.1080/00958972.2015.1043908

Accepted author version posted online: 23 Apr 2015.
Published online: 27 May 2015.

Journal of Coordination Chemistry, 2015
Vol. 68, No. 14, 2565–2585, http://dx.doi.org/10.1080/00958972.2015.1043908

Synthesis of monosodium salts of N-(5-nitro-salicylidene)-D-amino acid Schiff bases and their iron(III) complexes: spectral and physical characterizations, antioxidant activities

ÖZLEM ÖZDEMIR (NEE GÜNGÖR)*†, PERIHAN GÜRKAN†, MUSA SARI‡ and TUNCAY TUNÇ§

†Faculty of Science, Department of Chemistry, Gazi University, Ankara, Turkey
‡Faculty of Education, Department of Physics Education, Gazi University, Ankara, Turkey
§Department of Science Education, Science and Technology Application and Research Center, Aksaray University, Aksaray, Turkey

(*Received 19 January 2015; accepted 9 April 2015*)

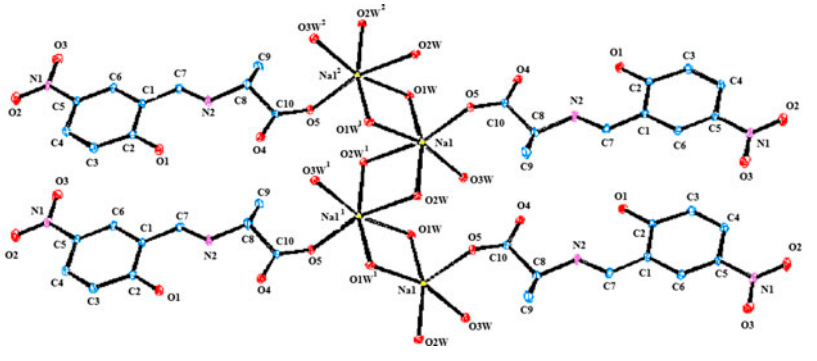

Amino acid Schiff bases, [NaL]·nH$_2$O (L = *N*-(2-hydroxy-5-nitrobenzylidene)alaninate, *N*-(2-hydroxy-5-nitrobenzylidene)valinate, and *N*-(2-hydroxy-5-nitrobenzylidene)phenylalaninate), were synthesized as monosodium salts (**L^{1}Na**–**L^{3}Na**). The structures of the monosodium salts were confirmed on the basis of elemental analysis, conductivity measurements, UV–vis, FT-IR, and 2D NMR (HMQC) spectroscopies. **L^{1}Na** was also structurally determined by single-crystal X-ray diffraction. Hydrogen bond between the amino N(2)–H and phenolate O(1) of the salicylidene part of the molecule played important roles in stabilizing the zwitterion crystal structure. The ranges of the D–H…A angles and those of the H…A and D…A distances indicated the presence of short hydrogen bonds in the structure. In addition, the monosodium salts have been evaluated for *in vitro* antioxidant activity. Iron(III) complexes (**L^{1}Fe**–**L^{3}Fe**) have been obtained by reaction of the appropriate ligand with iron(III) chloride in a 2 : 1 M ratio. Fe(III) complexes were characterized by elemental and thermal analysis, conductivity and magnetic susceptibility measurements, UV–vis, FT-IR, and X-ray photoelectron spectroscopy methods.

Keywords: Amino acid Schiff bases; Monosodium salts; Fe(III) complexes; X-ray; XPS; Antioxidant activity

*Corresponding author. Email: ozlemgungor@gazi.edu.tr

1. Introduction

Schiff bases obtained through condensation of amino acids with salicylaldehyde are model compounds of N-pyridoxylidene amino acid, a coenzyme of vitamin B_6. Various Schiff bases have been reported using DL-alanine and DL-valine [1], histidine, aspartic acid, glycine, cysteine, and glutamic acid [2]. Schiff bases and their transition metal complexes are important compounds in medicine with biological applications such as antibacterial [3, 4], antifungal [5, 6], antiviral [7, 8], analgesic [9, 10], anti-inflammatory [11, 12], and anticancer activities [13, 14]. These compounds have also been shown to be useful for chemosensor chemistry [15], catalysts for many organic reactions [16], effective catalysts in asymmetric synthesis [17], non-linear optical materials [18, 19], and luminescence materials [20].

The flavor, color, and nutritive properties of foods are changeable, related with lipid oxidation reactions. L-ascorbic acid, gallic acid, caffeic acid, uric acid, L-glutathione, and guercetin, etc. are used as antioxidants for maintaining quality of foods. A number of synthetic compounds have been presented in the literature for their antioxidant activity [21–23], but most of them are not soluble in water. In this work, we investigate the antioxidant activity of monosodium salts which are water soluble. 2,2-Diphenyl-1-picrylhydrazyl (DPPH) was used for determination of antioxidant activity because it reacts with an antioxidant directly and rapidly. This mechanism is based on the transfer of hydrogen from an antioxidant (AH) or a radical species ($R^{\cdot}$) to DPPH radical [24].

In this study, we have synthesized the monosodium salts and iron(III) complexes of the N-(5-nitro-salicylidene)-amino acids, where amino acid is D-alanine, D-valine, and D-phenylalanine. Single-crystal X-ray analysis of the monosodium salt $\mathbf{L^1Na}$, which has a functional side chain (alanine), shows that its crystals are 1-D coordination polymers. Each sodium ion has six coordination. The carboxylate of amino acid Schiff base coordinates Na^+ in a monodentate mode. Na^+ ions are linked by aqua bridges, …$Na(\mu\text{-}OH_2)_2Na$…

The structures of the newly synthesized compounds have been characterized by various spectroscopic techniques. The existence of intramolecular hydrogen bonding for the monosodium salts of amino acid Schiff bases has been studied both in solid state by FT-IR and X-ray crystallography and in the solution by UV–vis and NMR spectroscopies.

2. Experimental

2.1. *Materials and reagents*

D-alanine (Sigma), D-valine (Aldrich), D-phenylalanine (Sigma), 5-nitro-salicylaldehyde (Aldrich), sodium bicarbonate (Merck), iron(III) chloride (Aldrich), 2,2-diphenyl-1-picrylhydrazyl (DPPH) (Aldrich), and L-ascorbic acid (Carlo Erba) were used without purification. Absolute ethanol and methanol were purchased from Sigma.

2.2. *Instrumentation*

Melting points were determined on Barnstead Electrothermal BI 9200. Elemental analysis was performed on a LECO CHNS-932 analyzer. IR spectra from 4000 to 400 cm^{-1} were measured using KBr disks on a Mattson 1000 FTIR spectrophotometer. UV–visible spectra were obtained using an Analytika Jena UV-200 spectrophotometer at room temperature. Conductivity measurements were carried out in 1 mM solution using a WTW Series Inolab

Cond. 730 with a WTW Tetracon 325 electrode. $^{1}H/^{13}C$ NMR, 2D NMR (HMQC) spectra were obtained on a Bruker Ultrashield 300 MHz at room temperature. At room temperature, magnetic susceptibilities of Fe(III) complexes were determined using a Sherwood Scientific MKI model Evans magnetic balance calibrated with $Hg[Co(NCS)_4]$. The TGA-DTA curves of complexes were recorded using a SII 7300 EXSTAR between 35 and 800 °C at a heating rate of 10 °C min^{-1} in a N_2 atmosphere. XPS determination was carried out with a Thermo K-Alpha spectrometer. The X-ray source is Al Kα X-rays (monochromatic), carried out at 90° electron take-off angle. The experiments were conducted at pressures below 10^{-7} mbar.

2.2.1. X-ray structure determination of L^1Na. Crystallographic data of monosodium salt **L^1Na** were recorded on a Bruker APEX 2 CCD X-ray diffractometer employing plane graphite monochromated with MoK_α radiation ($\lambda = 0.71073$ Å) using $\omega-2\theta$ scan mode. The structures were solved by direct methods and refined by full-matrix least-squares techniques on F^2 using SHELXS-97 and refined using SHELXL-97 [25]. The empirical absorption corrections were applied by the multi-scan method via Bruker, SADABS software [26]. Hydrogens of water were located in difference Fourier syntheses with distances of O–H = 0.79(3)–0.90(3) Å. The remaining hydrogens were placed geometrically at distances of 0.86–0.96 Å from their parent for N–H and C–H bonds. ORTEP-3 for windows [27] and OLEX2 [28] drawing of the molecule with 40% probability displacement thermal ellipsoids and atom-labeling scheme are shown in figures 6 and 7, respectively.

2.3. *Synthesis*

2.3.1. Synthesis of monosodium salts of amino acid Schiff bases. Sodium bicarbonate (1.00 mmol, 0.0840 g) was added to an aqueous solution (10 mL) of the D-amino acid (1.00 mmol), and the mixture was stirred for 30 min. After completion of CO_2 evolution, the warm solution of 5-nitrosalicylaldehyde (1.00 mmol, 0.1540 g) in 15 mL absolute EtOH was added dropwise with stirring to an aqueous solution. There action was allowed to proceed for three days at 25 °C with stirring. The solvent was removed by rotary evaporator until an orange precipitate was formed. The solid products were purified by recrystallization from H_2O/EtOH mixture.

2.3.2. Synthesis of Fe(III) complexes. The monosodium salt of amino acid Schiff base (1 mmol) was dissolved in water (30 mL). The aqueous solution of iron(III) chloride (1 mmol, 10 mL) was added dropwise to solution of the ligand. The reaction mixture was stirred for one day at 25 °C. The mixture was kept over a period of 2–5 days at room temperature. The solid product was filtered and crystallized from H_2O/EtOH mixture.

2.4. *Antioxidant activity (DPPH UV–vis assay)*

DPPH UV–vis assay was based on the reported method [29, 30]. 0.1 mM methanolic solution of DPPH was prepared. A volume of 1 mL of 0.1 mM DPPH was added to different volumes of the aqueous or methanolic sample solutions (1 mg mL^{-1}). The mixture was shaken vigorously and incubated at room temperature for 30 min in the dark. The color of the solution turned from violet to pale yellow during antioxidant action. The absorbance of the samples was measured at 517 nm. Methanol was used for the baseline correction.

Ascorbic acid was used as standard. The free radical scavenging activity was calculated using the following formula (1), and the values were expressed as SC_{50} (mg sample per mL), the concentration of the samples that causes 50% scavenging of DPPH radical

$$\text{Radical scavenging activity}\,(\%) = \frac{[A_c - A_s]}{A_c} \times 100 \quad (1)$$

where A_c was the absorbance of the control (without any compound, only methanolic solution of DPPH), and A_s was the absorbance of the samples. All experiments were carried out in triplicate.

3. Results and discussion

3.1. *Structures of the ligands and the complexes*

The monosodium salts of amino acid Schiff bases have been synthesized by reaction of 5-nitro-salicylaldehyde with D-amino acids in the presence of sodium bicarbonate. The elemental analyses show 1 : 1 (Na : ligand) stoichiometry for these compounds, corresponding with $[NaL]\cdot nH_2O$ (L = *N*-(2-hydroxy-5-nitrobenzylidene)alaninate, *N*-(2-hydroxy-5-nitrobenzylidene)valinate, and *N*-(2-hydroxy-5-nitrobenzylidene)phenylalaninate). The proposed molecular formulas of the monosodium salts are given in scheme 1.

The mononuclear iron(III) complexes have been derived from chiral tridentate monosodium salts having imino–amino acid moiety. The elemental analyses confirm Na $[FeL_2]\cdot nH_2O$ formulation of the complexes. Fe(III) is bonded to two ligands through the imine nitrogen, carboxylate oxygen, and phenolate oxygen in a six-coordinate geometry. The proposed molecular formulas of the Fe(III) complexes are shown in scheme 2.

Analytical, physical, conductivity, and magnetic susceptibility values of the compounds are presented in table 1. All of the compounds are stable in air; the monosodium salts are soluble in water and polar organic solvents; iron(III) complexes are less soluble in water, but soluble in polar organic solvents.

Depending on the position of the hydrogen in this O…H…N bond, the o-hydroxy Schiff bases exhibit three tautomeric forms, as shown in scheme 3, the phenol-imine (A), zwitterionic (B), and keto-amine (C). On the basis of various spectroscopic techniques, it can be

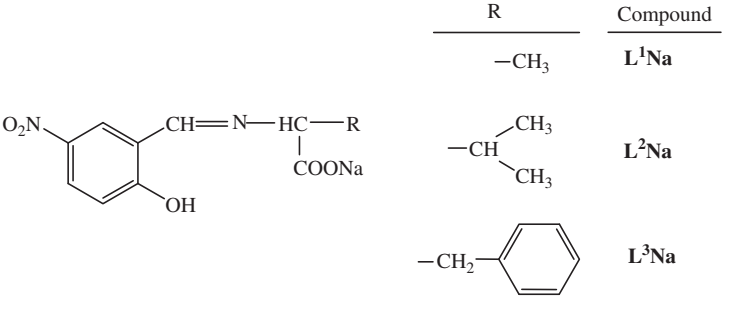

Scheme 1. Structures of the amino acid Schiff bases: **L[1]Na**: monosodium *N*-(2-hydroxy-5-nitrobenzylidene)alaninate; **L[2]Na**: monosodium *N*-(2-hydroxy-5-nitrobenzylidene)valinate; and **L[3]Na**: monosodium *N*-(2-hydroxy-5-nitrobenzylidene)phenylalaninate.

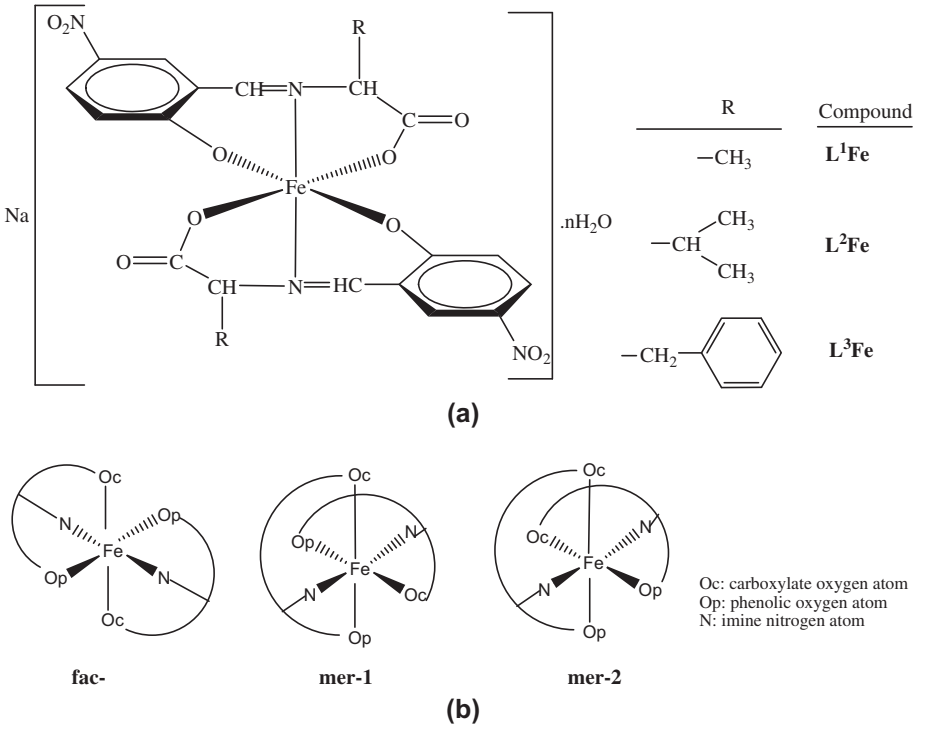

Scheme 2. (a) Suggested structures of Fe(III) complexes, (b) stereoisomers of the complexes.

concluded that salicylaldimine Schiff bases form mainly phenol-imine structures [31, 32]. In contrast to this, Schiff bases derived from 5-nitro-salicylaldehyde and aliphatic amines exist as almost pure keto-amine form [33] or the zwitterionic form [34]. Naphthaldimine Schiff bases exhibit either keto-amine structure or mixture of two tautomers [35].

3.1.1. IR spectra. Selected FT-IR absorption bands are given in table 2. Monosodium salts **L^2Na** and **L^3Na** show a broad band at 3420–3423 cm^{-1}, which is due to *ν*OH. The azomethine (C=N) band can be accountable partially for the phenol-imine form which is inferred from IR spectra [36]. Both observation of the (OH) band and the existence of the *ν*(C=N) at 1646–1659 cm^{-1} are evidence for the phenol-imine form of two monosodium salts in the solid state. The band at 3240 cm^{-1} and a broad band at 1830–2362 cm^{-1} centered at 2129 cm^{-1} are assigned to (*ν*NH) and (*ν*NH^+) vibrations, respectively, for **L^1Na** (figure 1). These bands prove that **L^1Na** exists as a zwitterionic form by the presence of ionic N^+–H…O^- hydrogen bonds. Bands at 1607–1619 cm^{-1} and 1383–1404 cm^{-1} are attributed to the asymmetric and symmetric stretches of carboxylate, respectively [37]. Bands at 1538–1543 and 1322–1336 cm^{-1} are ascribed to $\nu(ONO^-)_{as}$ and $\nu(ONO^-)_s$ stretches, respectively.

IR spectra of Fe(III) complexes are compared with the monosodium salts in order to determine the coordination sites that may be involved in chelation. The phenolic *ν*(C–O) stretch is at 1222–1231 cm^{-1} for monosodium salts **L^1Na-L^3Na**. In all Fe(III) complexes,

Table 1. Analytical and physical data of the compounds.

Comp.	Empirical formula (molecular weight)	Color yield (%)	m.p. (°C)	Found (Calcd) % C	H	N	Fe	μ_{eff} (BM)[a]	Λ (Ω^{-1} cm^2 mol^{-1}) 22.5 ± 0.5 °C	24.0 ± 0.5 °C
L^1Na	$[NaC_{10}H_9N_2O_5]\cdot 3H_2O$ (314.2269 g mol^{-1})	Yellow 83	270	38.13 (38.22)	4.75 (4.81)	8.73 (8.92)	–	–	89.0[b]	105.1[b]
L^2Na	$[NaC_{12}H_{13}N_2O_5]\cdot 3H_2O$ (342.2805 g mol^{-1})	Dark yellow88	222–226[c,d]	41.98 (42.11)−	5.23 (5.60)	8.24 (8.18)	–	–	82.9[b]	89.6[b]
L^3Na	$[NaC_{16}H_{13}N_2O_5]\cdot 3H_2O$ (390.3245 g mol^{-1})	Orange 94	121–128[c]200[d]	49.31 (49.24)−	4.78 (4.91)	7.22 (7.18)	–	–	87.8[b]	92.9[b]
L^1Fe	$Na[Fe(C_{10}H_8N_2O_5)_2]\cdot H_2O$ (569.2192 g mol^{-1})	Reddish black 70	>360	43.59 (42.20)	3.772 (3.19)	8.768 (9.84)	9.83[e](9.81)	5.01	79.1[f]	82.7[f]
L^2Fe	$Na[Fe(C_{12}H_{12}N_2O_5)_2]\cdot 3H_2O$ (661.3568 g mol^{-1})	Reddish black 79	>360	42.64 (43.59)	4.166 (4.57)	8.142 (8.47)	8.23[e](8.44)	5.18	30.9[f]	34.6[f]
L^3Fe	$Na[Fe(C_{16}H_{12}N_2O_5)_2]\cdot 2H_2O$ (739.4296 g mol^{-1})	Reddish black 75	>360	51.66 (51.98)	3.986 (3.82)	7.827 (7.58)	7.66[e](7.56)	5.94	23.0[f]	26.8[f]
								H_2O	2.3	2.4
								DMSO	0.2	0.3
								0.01 M KCl	1283	1401

[a]At room temperature.
[b]In 1 mM aqueous solution.
[c]Foaming point.
[d]Decomposition point.
[e]Calculated using thermogravimetric data.
[f]In1 mM DMSO solution.

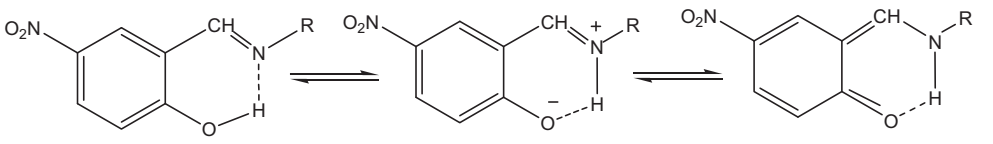

Scheme 3. The tautomeric equilibria in ortho-hydroxy Schiff bases.

this band is observed at 1095–1097 cm^{-1}, confirming involvement of the phenolic group in complex formation. The medium broad bands at 3411–3424 cm^{-1} are assigned to ν(OH) of coordinated water. ν(C=N) vibrations of complexes are at 1633, 1625, and 1627 cm^{-1} for **L^1Fe**, **L^2Fe**, and **L^3Fe**, respectively. This band shifts to lower frequencies on complex formation, indicating coordination of the azomethine N to Fe^{+3}. New absorptions at 460–465 cm^{-1} are assigned to ν(Fe–N). Furthermore, vibrations of ν(Fe–O) are 498–503 cm^{-1}. $\nu(COO–)_{as}$ and $\nu(COO–)_s$ vibrations are at 1605–1606 cm^{-1} and 1383–1386 cm^{-1}, respectively. Δ(vas-vs) of 220–222 cm^{-1} is characteristic of a monodentate carboxylate [38, 39]. The shift to lower frequency by 2–13 cm^{-1} in the metal complexes suggests coordination of carboxylate oxygen to Fe^{+3}, supported by appearance of new ν(M−OOC) bands at 654–655 cm^{-1}. The bands at 1558–1561 cm^{-1} and 1312 cm^{-1} are related to the $\nu(ONO)_{as}$ and $\nu(ONO)_s$ stretches, respectively.

3.1.2. UV–visible spectra. Although the UV–vis spectrum of salicylaldimine Schiff bases indicates a band at <400 nm, naphthaldimine Schiff bases show a new band at >400 nm [32].

Electronic spectral data of all the compounds are listed in table 2. In water, the absorption spectra of the monosodium salts show two high energy bands at 349–354 nm and 381–385 nm (figure 2). These bands are assigned to π–π* and n–π* transition of the (C=N) group, respectively [40]. This result proposes that the compounds exist in either the phenol-imine or zwitterionic form in water.

Fe(III) complexes exhibit a band at 470 nm in DMSO. This band belongs to the charge transfer transition (LMCT) from a filled (pπ) orbital of the phenolate oxygen to the half-filled (dπ*) orbital of the Fe(III) ion [41] and is responsible for the dark red color of the complexes. The higher energy shoulder at 398–405 nm is a superposition of the carboxylate-to-Fe(III) and imino-to-Fe(III) charge transfer bands. Thereupon, the band around 337 nm is attributed to π–π* transition of the (C=N) group.

3.1.3. Conductivity and magnetic susceptibility measurements. The molar conductance values of the monosodium salts measured in 1 mM aqueous solution are at 82–89 and 89–105 $Ohm^{-1}cm^2\ mol^{-1}$ at different temperatures, indicating their 1 : 1 electrolytic behavior [42]. Fe(III) complexes are 1 : 1 electrolytes with the conductance values of 23–79 $Ohm^{-1}cm^2\ mol^{-1}$ and 26–82 $Ohm^{-1}cm^2\ mol^{-1}$ in 1 mM DMSO solution. It suggests that two ligand ions (L^{-2}) are in the coordination sphere and sodium ion is uncoordinated, corresponding with $Na[FeL_2]$.

The mononuclear Fe(III) complexes show a magnetic moment (μ_{eff}) of 5.01–5.94 BM. According to the magnetic moment calculations, the complexes have five unpaired electrons and are paramagnetic, which is expected for octahedral high-spin d^5 Fe(III) (5.90 BM).

Table 2. FT-IR and UV–vis data of the compounds.

Comp.	H_2O	NH=NH^+	CH benzene	CH/CH_2	C=N	C=C	COO_{as} COO_s	ONO_{as} ONO_s	δCH	C–O	M-OOC M-O	M-N	UV–vis (nm) (log ε)
L^1Na	3423.0	3239.8	3061.7	2989.9	1659.0	1638.3	1607.5	1540.4	1447.0	1231.7	–		354[a] (3.55), 384 (3.53)
		1829.7–2361.6		2926.3		1484.8	1404.3	1336.9	1372.0				
L^2Na	3420.9	Not obs.	3064.5	2963.3	1656.7	1474.9	1619.2	1538.7	1445.5	1230.6	–		350[a] (3.34), 381 (3.28)
		Not obs.		2880.2			1387.0	1328.0					
L^3Na	3422.5	Not obs.	3063.2	2925.8	1646.6	1511.4	1610.9	1543.6	1444.1	1222.8	–		349[a] (3.28), 385 (3.22)
		Not obs.					1383.7	1322.4					
L^1Fe	3424.7	–	3034.4	2918.0	1633.8	1497.7	1606.3	1561.6	1463.5	1097.3	654.9	465.8	337[b] (3.51), 405sh (2.95),
							1386.8	1312.8			503.8		473 (2.59)
L^2Fe	3411.0	–	3069.7	2965.7	1625.4	1499.5	1606.0	1558.1	1462.5	1097.7	655.4	460.4	344[b] (3.49), 402sh (3.19),
				2928.6			1386.0	1312.2			502.9		477sh (2.68)
L^3Fe	3411.0	–	3062.3	2921.5	1627.6	1499.2	1605.4	1559.1	1459.0	1095.8	654.1	464.8	344[b] (3.60), 398sh (3.38),
							1383.6	1312.1			498.0		483sh (2.76)

[a]In 1 mM aqueous solution.
[b]In 1 mM DMSO solution.

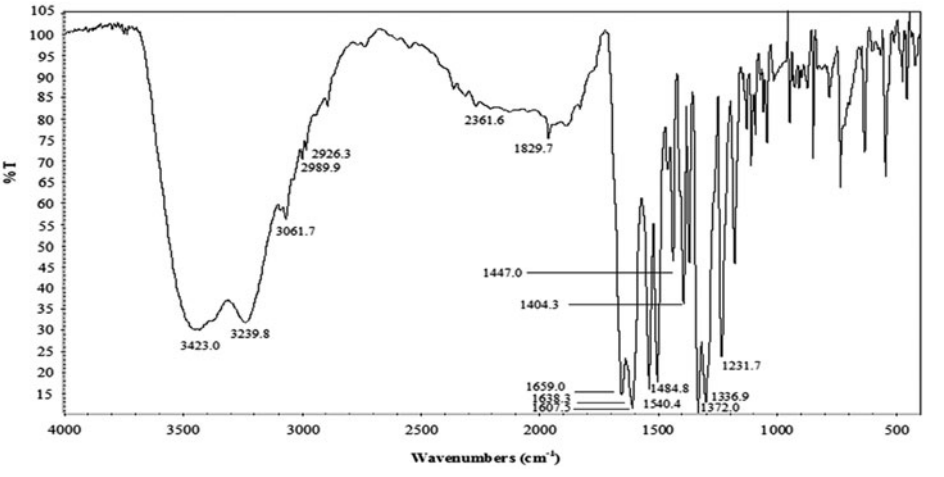

Figure 1. IR spectra of **L[1]Na**.

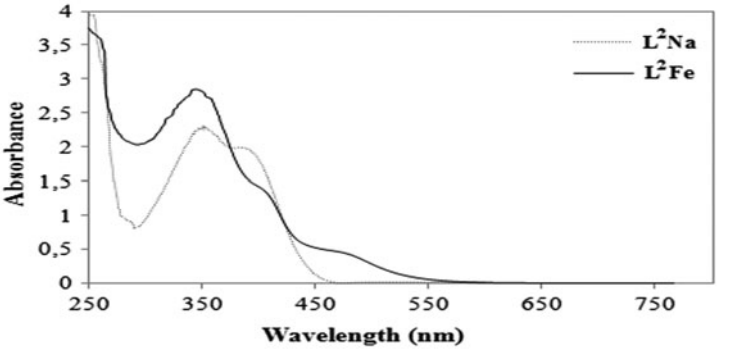

Figure 2. UV–vis spectra of **L[2]Na** in D_2O and **L[2]Fe** in DMSO.

3.1.4. NMR spectra. ^{1}H NMR data in D_2O for the monosodium salts are summarized in table 3. The peak assignments are achieved on the basis of ^{1}H-^{13}C 2D NMR (HMQC) spectra of **L[1]Na** in D_2O.

The OH (H-8) proton is at 9.85–9.90 ppm [43]. The imine (H-1) proton is at 8.25–8.38 ppm as a singlet for **L[1]Na** and **L[2]Na** and a doublet ($^3J_{NHCH}$ = 2.63 Hz) for **L[3]Na**. Furthermore, the OH and the (CH=N) protons of **L[1]Na** shift downfield by 0.16–0.21 ppm and 0.27–0.40 ppm in DMSO-d6, respectively. Aromatic protons resonate at 6.40–6.54 ppm (H-4), 7.80–8.03 ppm (H-5) and 7.95–8.30 ppm (H-7). In addition, the multiplet signals from 7.10 to 7.30 ppm (m, J = 7.34 Hz) are due to benzene protons for **L[3]Na**.

The ^{1}H NMR spectra show largest splitting of (H-10) signal in the aliphatic region into two peaks, which proves the isomeric impurity of the monosodium salts. The compounds occur in two diastereomeric forms (D- and L-). Both diastereomers are observed in a

Table 3. ^{1}H chemical shifts of the monosodium salts in D_2O (ppm).

	Number								
Comp.	1	2 3 6 9	4	5	7	8	10	11	12,1 2*
L^{1}Na	8.38 (s,1H)	– –	6.48(d) J = 9.563	7.95(d-d) J = 9.652	8.22(d) J = 2.989	9.90 (s,1H)	3.65(q) J = 7.237	1.37(d) J = 7.235	
		– –	6.54(d) J = 9.737 Σ = 1H	8.03(d) J = 2.920 Σ = 1H	8.30(d) J = 3.111 Σ = 1H		4.32(q) J = 7.144 Σ = 1H	1.54(d) J = 7.173 Σ = 3H	
	8.65 [a](s,1H)	– – – –	6.17(d) J = 9.713 6.45(d) J = 9.716 Σ = 1H	7.75(d) 7.95(d-d) J = 9.794 Σ = 1H	8.17(s) 8.40(d) J =3.031 Σ = 1H	10.06 (s,1H)	3.95(d, 1H) J = 6.911	1.25(d) J = 7.008 1.45 (d) J = 7.088 Σ = 3H	
L^{2}Na	8.30(s,1H)	–	6.40(d) J = 9.564 6.50(d) J = 9.696 Σ = 1H	7.85(d-d) J = 9.555 7.93(d-d) J = 9.676 Σ = 1H	8.15(d,1H) J = 2.712	9.85 (s,1H)	3.50(s) 4.05(s) Σ = 1H	2.15(m) J = 4.436 2.30(m) J = 6.873 Σ = 2H	0.90(q) J = 7.082 Σ = 6H
L^{3}Na	8.25(d,1H) J =2.627[b]	–	6.46(d-d,1H) J = 9.551	7.80(s) Σ = 1H	7.95(d,1H) J = 8.504	9.85 (s,1H)	3.85(q) J = 5.216 4.38 (q) J = 4.344 Σ = 1H	2.95–3.18 (m) J =7.267 3.30(d-d) J = 13.959 Σ = 2H	7.10–7.30 (m,5H) J = 7.341

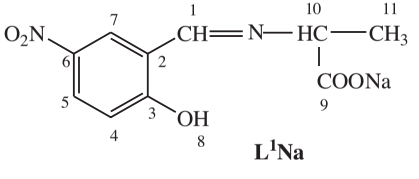

L^{1}Na

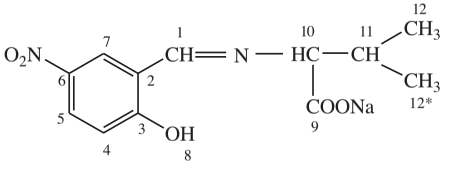

L^{2}Na

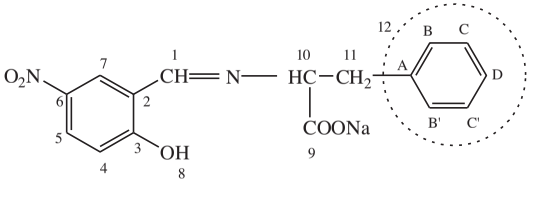

L^{3}Na

[a]DMSO-d_6 [b]J, coupling constant.

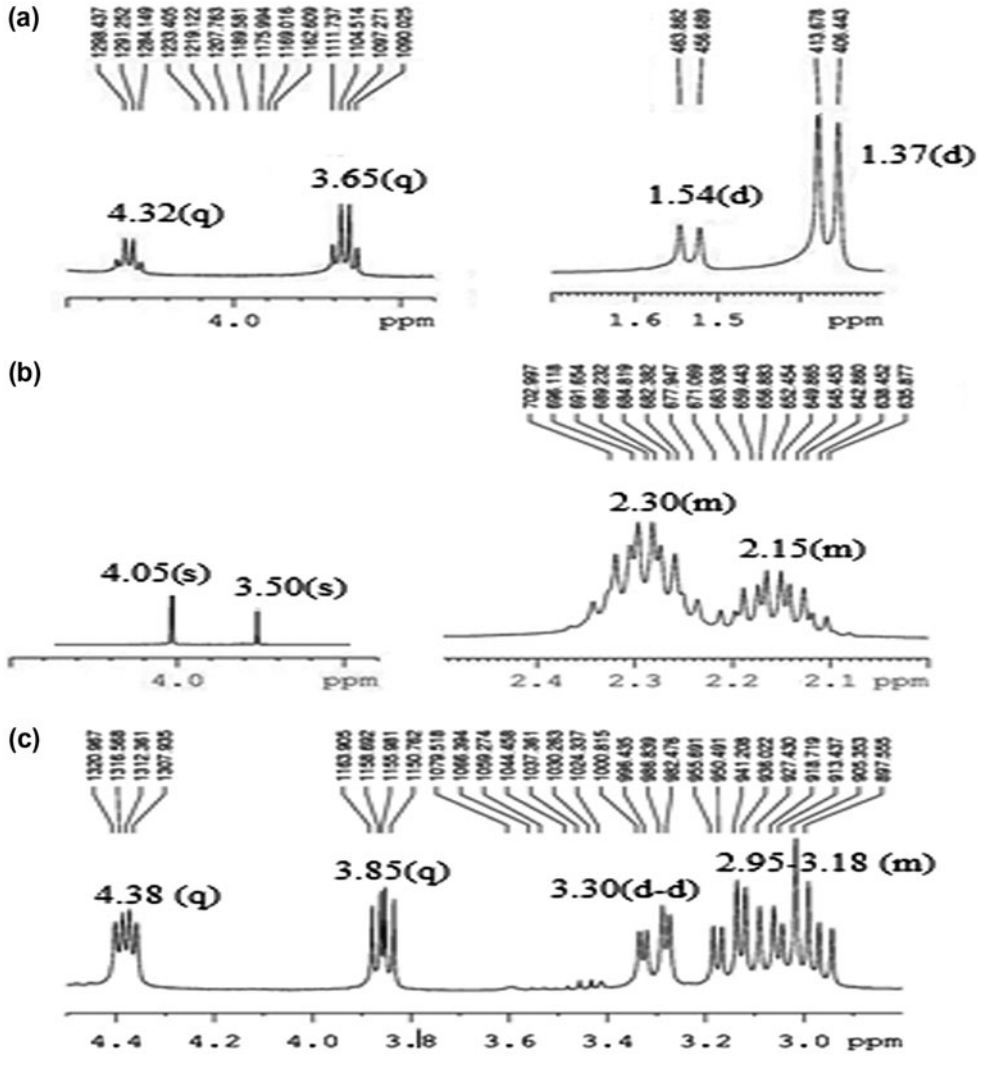

Figure 3. The aliphatic ^{1}H signals of the monosodium salts in D_2O; (a) **L^1Na**, (b) **L^2Na**, and (c) **L^3Na**.

1 : 2.5, 1 : 0.7, and 1 : 1.5 ratios for **L^1Na**, **L^2Na,** and **L^3Na**, respectively (figure 3). The diastereomeric ratio is calculated from the signals for the (H-10) protons. Diastereotopic (H-11) protons give two peaks as doublets for **L^1Na** and multiplets for **L^2Na** and **L^3Na**. Although H-12 is diastereotopic, only one signal has been observed at 0.90 ppm (quartet) for **L^2Na**.

The proton de-coupled ^{13}C NMR data for the monosodium salts are listed in table 4. According to the ^{13}C NMR spectra of the compounds, the signal at 166.32–166.98 ppm is ascribed to the imine (C-1) carbon [31]. The signal at 174.26–182.5 ppm is assigned to the phenolic (C-3) carbon. Furthermore, the carboxylate (C-9) carbon is observed at 193.56–195.6 ppm. Chemical shifts from 113 to 136 ppm are for the aromatic carbons. The

Table 4. ^{13}C chemical shifts of the monosodium salts in D_2O (ppm).

Comp.	Number											
	1	2	3	4	5	6	7	8	9	10	11	12,1 2*
L^1Na	166.8[a]	114.0	177.5 178.1 181.4 182.5	124.3 125.1	132.8	135.8 136.2	129.7	–	195.6	51.5 61.8	17.3 18.9	
	166.08[b]	118.90	n/o[c]	122.65	131.12	140.24	124.84	–	189.49	n/o	n/o	
L^2Na	166.98[d]	113.43	174.56 175.04 179.88 180.49	123.30 123.35	131.21	133.82 133.93 134.77	128.53	–	193.57	60.55 71.89	29.27 31.60	16.47 16.76 18.11 18.70
L^3Na	166.32[d]	113.10	174.26 174.51 179.75 180.27	123.11 123.24	131.05 131.15	133.66 133.89 134.54	127.61	–	193.56	56.11 67.35	36.54 39.29	A, 143.71 B, 135.23 B′, 135.78 C, 128.91 C′, 129.65 D, 124.05

[a]HMQC/^{13}C NMR data.
[b]DMSO-d_6.
[c]Not observed.
[d]^{13}C NMR data.

nitro group causes the greatest downfield shift to 133.66–136.2 ppm for C-6 when compared to hydrogen as the substituent in the benzene ring. As expected, alkyl carbons (C-10, C-11, and C-12) are observed between 17 and 71 ppm.

3.1.5. Thermogravimetric analyses. The thermoanalytical data of Fe(III) complexes are given in table 5. The TGA curves show that thermal decomposition of the complexes takes place in two steps as illustrated in figure 4(a)–(c). The first mass loss at 40–171 °C is due to escape of the uncoordinated water molecules. Second thermal reaction which is related to decomposition of the organic ligands starts at 162 °C and continues to 738 °C. DTA peaks appear at 214–270 °C. O_2 was added to the medium at 762 °C, and formation of the metal oxide was observed.

Table 5. Thermal data of Fe(III) complexes.

Comp.	Process	Temp. °C	Product/residue	% Mass	
				Calcd	Found
L^1Fe	Dehydration Decomposition	41–109 162–738 DTA peak 269 (endoth.)	1 mol H_2O Fe_2O_3	3.16 28.06	3.15 28.13
L^2Fe	Dehydration Decomposition	40–171 183–731 DTA peak 214 (endoth.) 262 (endoth.)	3 mol H_2O Fe_2O_3	8.17 24.15	7.88 23.56
L^3Fe	Dehydration Decomposition	46–154 181–719 DTA peak 270 (endoth.) 629 (exoth.)	2 mol H_2O Fe_2O_3	4.87 21.60	5.0 21.88

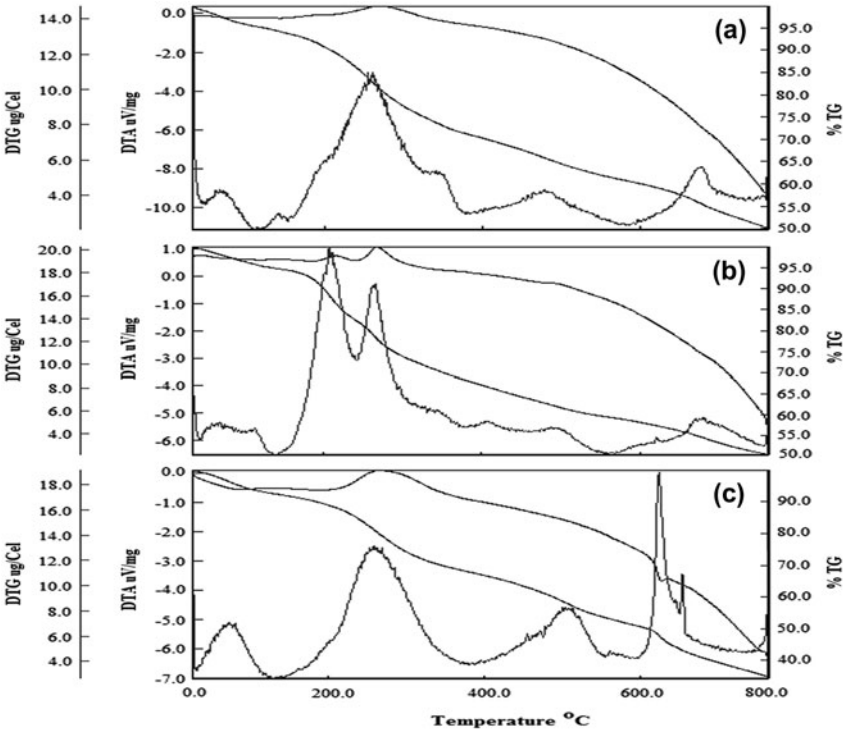

Figure 4. The TGA curves of (a) $\mathbf{L^1Fe}$, (b) $\mathbf{L^2Fe}$, and (c) $\mathbf{L^3Fe}$.

3.1.6. XPS spectra. The values of the metal electron binding energy (BE) in the complexes are important to analyze the coordination model. Fe(III) complexes have been characterized by X-ray photoelectron spectra (XPS). C1s, N1s, O1s, Na1s, and Fe2p bands of the complexes are approximately the same and are listed in table 6.

The XPS spectra of the complexes in the C1s region have been deconvoluted to four components, except $\mathbf{L^2Fe}$ with five peaks. The peak at 284 eV is assigned to carbons of aromatic C=C and alkyl C–C; the peak at 285 eV is attributed to the C–N and C–O carbons and the peak at 288 eV is connected with the carboylate carbon [44]. The peak at 286 eV belongs to the azomethine (C=N) carbon [45].

The N1s peak of the complexes has been deconvoluted to three or four components. The component at 406 eV indicates the nitro group, which is not reduced by such a short X-ray exposure [46] for $\mathbf{L^3Fe}$. In contrast, this component has not been observed in the N1s XPS spectra of $\mathbf{L^1Fe}$ and $\mathbf{L^2Fe}$. For all the complexes, peaks with higher binding energies (404–405 eV) can be ascribed to chemisorbed nitrogen oxides (i.e. nitrite and nitrate) [47]; the peaks at *ca.* 400–401 eV may be assigned to nitrogen in a lower oxidation state (Ar–N=O) [48]. The (C–N) and (C=N) species correspond to peak components with BE at 398 eV [49] for $\mathbf{L^1Fe}$ and $\mathbf{L^3Fe}$. For $\mathbf{L^2Fe}$, although the binding energy value of (C–N) peak has been observed at 398.78 eV, the peak at 399.48 eV can be marked to (C=N) [44] or (Ar–NH_2) [48].

The O1s peak of all the complexes has been deconvoluted to three components. The first component at 531 eV can be associated to oxygen of phenolic ($C–O^-$), which is

Table 6. The data of XPS spectra of Fe(III) complexes.

Comp.	C1s B.E. (eV)	C1s Species	N1s B.E. (eV)	N1s Species	O1s B.E. (eV)	O1s Species	Na1s	Fe(III) $Fe2p_{1/2}$	Fe(III) $Fe2p_{3/2}$
L^1Fe	284.38	C-C, C=C[a]	398.88	C-N, C=N	531.58	C-O	1071.38	724.48	710.78
	285.58	C-N, C-O	401.28	Ar-N=O	532.68	C=O			
	286.08	C=N	405.08	NO_3[b]	533.28	Ar-N=O			
	288.38	COO^-							
L^2Fe	284.18	C-C, C=C[a]	398.78	C-N	531.28	C-O	Not determined	724.08	710.48
	285.18	C-N	399.48	Ar-NH_2, C=N	533.28	C=O			
	285.78	C-O	400.48	Ar-N=O	534.18	Ar-N=O			
	286.28	C=N	404.98	NO_3[b]					
	288.18	COO^-							
L^3Fe	284.58	C-C, C=C[a]	398.88	C-N, C=N	531.58	C-O	1071.48	723.68	710.78
	285.88	C-N, C-O	401.18	Ar-N=O	533.18	C=O			
	286.28	C=N	404.88	NO_3[b]	534.58	Ar-N=O			
	288.08	COO^-	406.38	Ar-NO_2					

[a]Aryl.
[b]Chemisorbed nitrogen oxides.

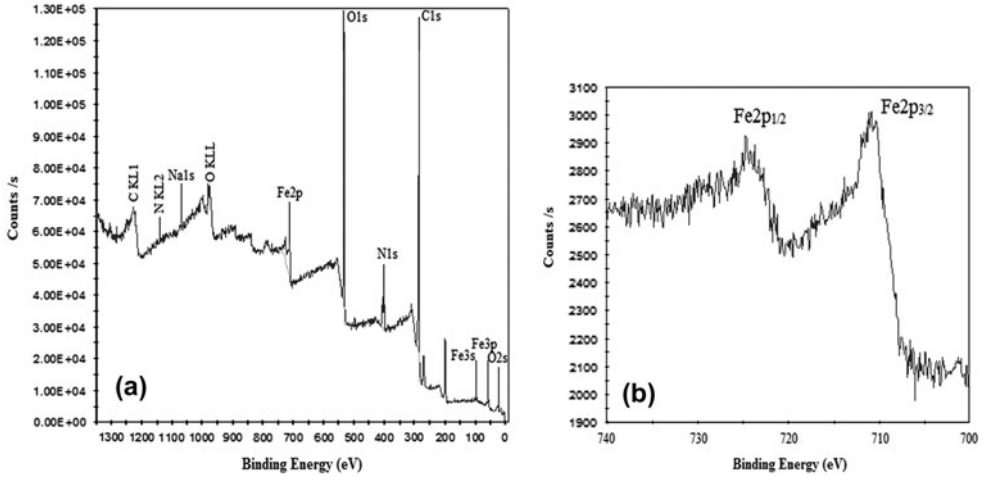

Figure 5. The XPS spectra of **L^1Fe** in (a) C1s, O1s, N1s, and Na1s region and (b) $Fe2p_{1/2}$ and $Fe2p_{3/2}$ region.

coordinated with Fe(III). The second component between 532 and 533 eV can be related to oxygen in carboxylate (COO^-) coordinated with Fe(III) [49]. The peak at 534 eV may be due to (Ar–N=O) group.

The Na1s spectra of **L^1Fe** and **L^3Fe** show a component at 1071 eV. This value agrees very well with reported data [50].

The XPS peaks of $Fe2p_{3/2}$ and $Fe2p_{1/2}$ for **L^1Fe** are shown in figure 5(b). The peak positions of $2p_{1/2}$ and $2p_{3/2}$ depend on the ionic states of iron. For Fe(III), the area of $Fe2p_{3/2}$ peak is greater than that of $Fe2p_{1/2}$ because of spin–orbit (j–j) coupling. In agreement with

the literature data [49, 51], the XPS peaks of $Fe2p_{3/2}$ and $Fe2p_{1/2}$ are observed at BE values at 710 and 724 eV, respectively. This result suggests that iron has +3 valency for **L[1]Fe-L[3]Fe**, as expected.

3.1.7. Crystal structure of monosodium salt L[1]Na. The molecular structure of **L[1]Na**, with the atom labeling of symmetric and asymmetric units, is shown in figures 6 and 7. The crystal and instrumental parameters used in the unit-cell determination and data collection are summarized in table 7, and selected bond lengths and angles are listed in table 8.

The monosodium salt **L[1]Na**, $[NaC_{10}H_9N_2O_5]\cdot 3H_2O$, crystallizes in the monoclinic, P $2_1/c$ space group. The compound has a center of symmetry at Na1. In the symmetric unit, the coordination environment of the Na1 ion has a distorted octahedral configuration coordinated by carboxylate O5 and five water molecules (O1w, O2w, O3w, $O1w^1$, and $O2w^2$). The symmetric unit contains three (Na1, $Na1^1$, $Na1^2$) ions and nine coordinated water molecules. The coordination arrangement is characterized by an $O5–Na1–O2w^2$ equatorial angle 164.59(7) Å. The $Na1…Na1^1$ and $Na1…Na1^2$ bridging bond distances are 3.3329(17) and 3.4969(17) Å, respectively. In the asymmetric unit, the Na1–O and Na1–Ow bond distances are 2.3305(19) Å and 2.2987(19)–2.433(2) Å, respectively.

The crystal structure contains intramolecular hydrogen bonds between the amino N(2)–H and phenolate O(1) of salicylidene, playing an important role in stabilizing the zwitterionic form. The compound has an intramolecular N–H…O hydrogen bond [O1–H2; 0.86, H2…N2; 1.97, N2…O1; 2.638(3) Å, N2–H2…O1 134.2°]. The ranges of the D–H…A angles and those of the H…A and D…A distances indicate the presence of short hydrogen bonds in the structure.

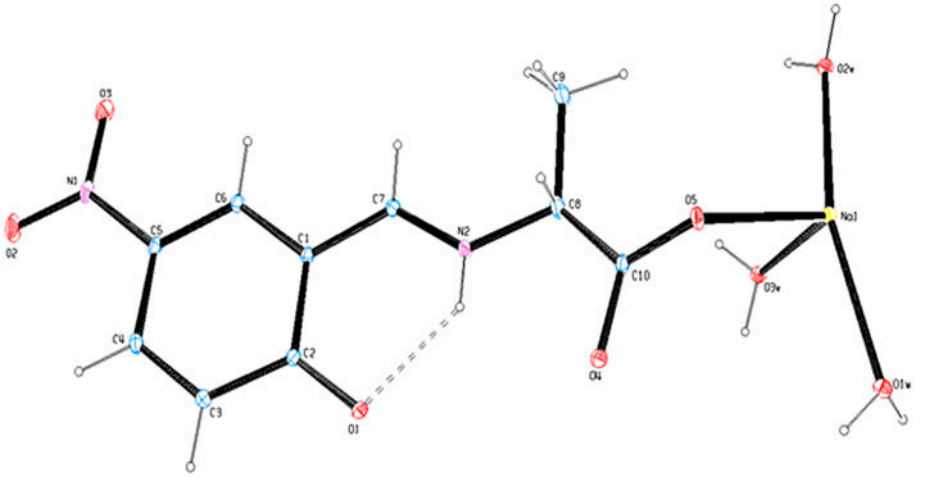

Figure 6. An ORTEP drawing of the asymmetric unit of compound with the atom-numbering scheme.
Notes: Displacement ellipsoids are drawn at the 40% probability level, and hydrogens are indicated as dashed lines.

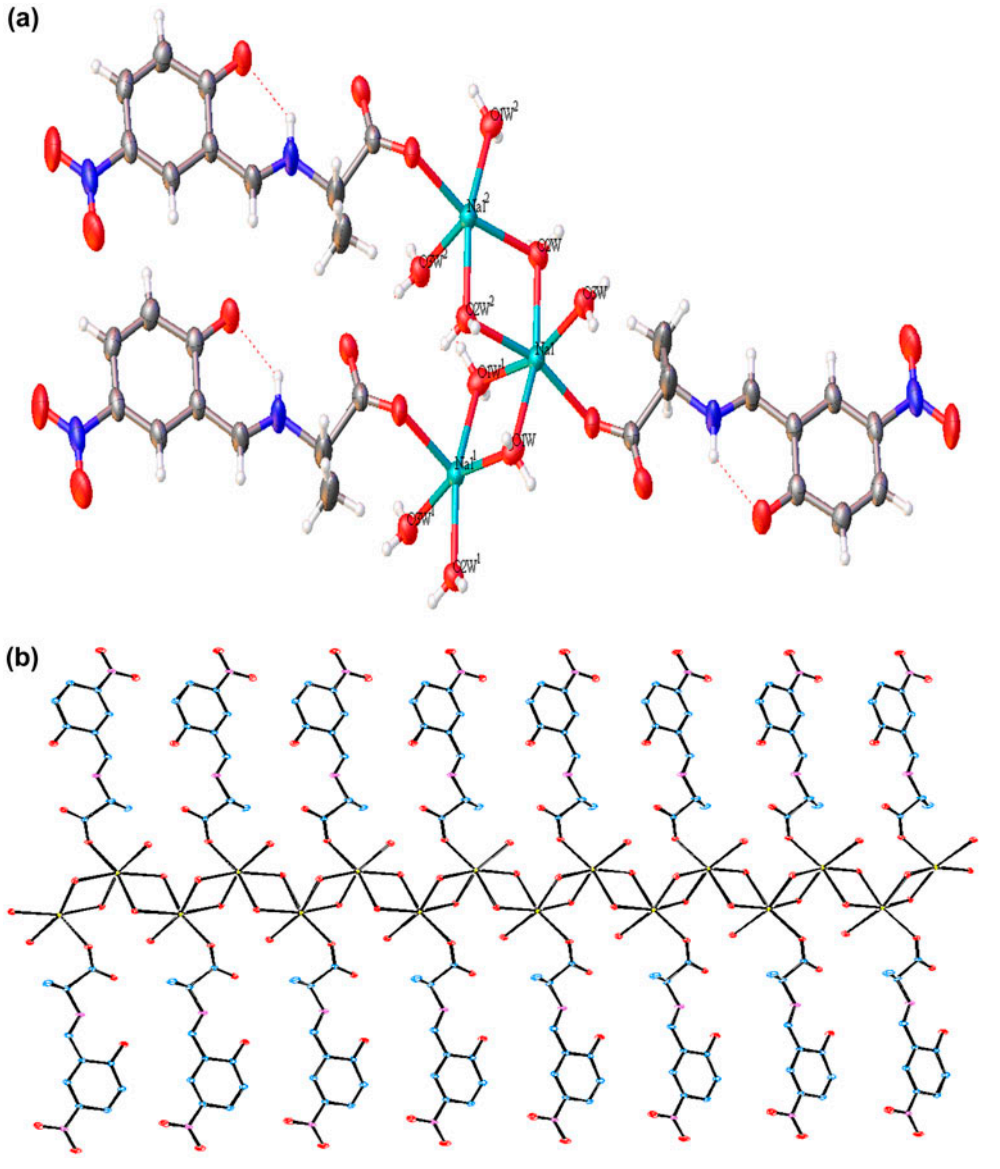

Figure 7. (a) The 1-D coordination polymer including symmetric unit in **L[1]Na**; (b) view of the zigzag infinite chains.

3.2. *Antioxidant activities*

The antioxidant activities of the monosodium salts have been determined using 2,2-diphenyl-1-picrylhydrazyl (DPPH). The results are summarized in table 9. DPPH scavenging activity of the monosodium salts are attributed to the presence of hydroxyl group. The hydroxyl groups of these compounds are H· donors, and DPPH is a hydrogen acceptor (or free radical scavenger), as shown in scheme 4.

Table 7. Crystal data and structure refinement details for **L^1Na**.

Chemical formula	$C_{10}H_{15}N_2O_8Na$
Formula weight	314.23
Temperature (K)	296(2)
Wavelength (Å)	0.71073
Crystal system, space group	Monoclinic, P 2_1/c
Unit-cell dimensions (Å, °):	
a	15.2817(4)
b	5.2590(10)
c	17.7991(5)
β	102.315(13)
Volume (Å^3)	1397.54(6)
Z	4
Absorption coefficient (mm^{-1})	0.154
Calculated density (Mg m^{-3})	1.493
F (000)	656
Crystal size (mm)	0.22 × 0.16×0.10
Theta range for data collection (°)	1.36–26.37
Limiting indices	$-19 \le h \le 19$, $-6 \le k \le 6$, $-22 \le l \le 22$
Reflections collected	30,996
Independent reflections	2860
Number of reflections used	2619
Number of parameters	219
Max. and min. transmission	0.978, 0.985
Refinement method	Full-matrix least-squares on F^2
Final *R* indices [$I \ge 2\sigma(I)$]	$R_1 = 0.0499$, $wR_2 = 0.1359$
R indices (all data)	$R_1 = 0.0537$, $wR_2 = 0.1395$
Goodness of fit (GOF) on F^2	1.052
Largest difference in peak and hole (e Å^{-3})	−0.478 and 0.785

Table 8. Selected bond distances (Å) and angles (°) for **L^1Na**.

Na1–O5	2.3305(19)	Na1–O1w^1	2.459(2)
Na1–O1w	2.433(2)	Na1–O2w^2	2.4848(19)
Na1–O2w	2.2987(19)	Na1–Na1^1	3.3329(17)
Na1–O3w	2.404(2)	Na1–Na1^2	3.4969(17)
O2w–Na1–O5	107.64(7)	O3w-Na1-O1w	97.67(7)
O2w–Na1–O3w	81.19(7)	O5-Na1-O2w^2	164.59(7)
O2w–Na1–O1w	161.15(8)	Na1-O1w-Na1^1	85.89(7)
O5–Na1–O1w	91.17(7)	Na1-O2w-Na1^2	93.87(7)
O5–Na1–O3w	97.91(7)	O2w-Na1-O1w^1	83.88(7)

Symmetry code: (1) $1-x, 1-y, 1-z$; (2) $1-x, 2-y, 1-z$.

Table 9. SC_{50} values for the monosodium salts.

	SC_{50} mg mL^{-1} (μM)	
Comp.	Methanol	Water
L^1Na	1.384 (4.405)	2.497 (7.947)
L^2Na	3.114 (9.098)	4.012 (11.721)
L^3Na	0.449 (1.150)	0.516 (1.322)
Ascorbic acid	<0.025 (0.142)	0.46 (2.612)

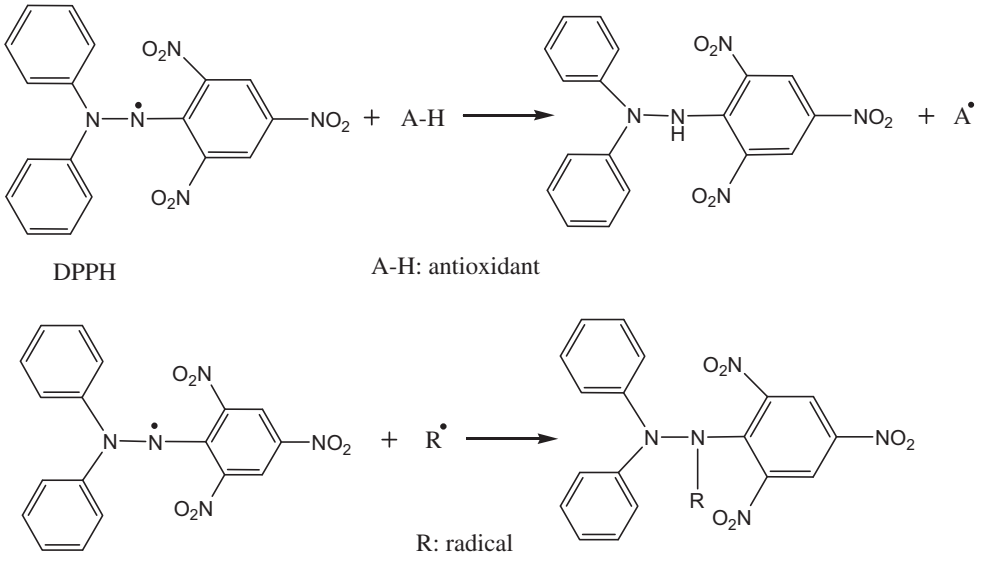

Scheme 4. The mechanism of DPPH radical.

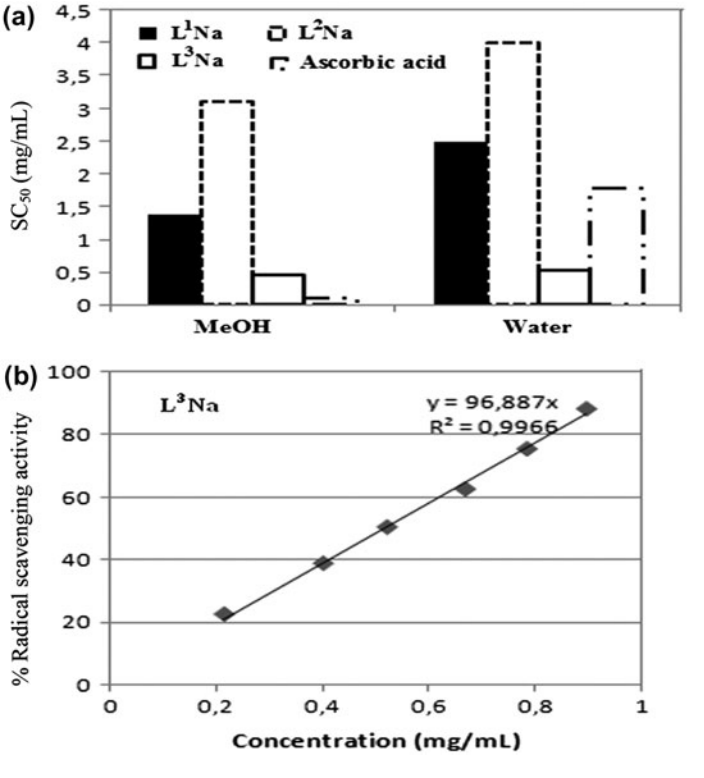

Figure 8. (a) Comparable chart for SC_{50} values of the monosodium salts; (b) effect of increasing amounts of **L^3Na** on the radical scavenging activity.

All of the monosodium salts show moderate antioxidant activity in methanolic solution. The SC_{50} values decrease **L^2Na** > **L^1Na** > **L^3Na** [figure 8(a)]. The SC_{50} value of ascorbic acid was < 0.025 mg/mL (0.142 μM) in methanolic solution. However, SC_{50} value of ascorbic acid was fairly low compared to those reported as 11.8 μM [52] and 42.4 μM [53].

The monosodium salts **L^1Na** and **L^2Na** are moderately active, and **L^3Na** has significant activity in aqueous solution. **L^3Na** with SC_{50} at 0.516 mg mL^{-1} (μM) possesses highest radical scavenging activity [figure 8(b)]. The SC_{50} value of ascorbic acid is 0.46 mg mL^{-1} (2.612 μM) in aqueous solution. The good activity of all the compounds may be related to the strong electron withdrawing group (NO_2) and the phenyl group for **L^3Na**.

4. Conclusion

The monosodium salts of amino acid Schiff bases have been synthesized by using 5-nitrosalicylaldehyde and D-amino acids in the presence of $NaHCO_3$. Iron(III) complexes were derived from the monosodium salts. The molecular structures have been determined by spectroscopic methods (FT-IR, UV–vis, NMR, XPS), conductivity, magnetic susceptibility measurements, elemental and thermal analyses. FT-IR spectra indicate that **L^2Na** and **L^3Na** exist as the phenol-imine form in the solid state, whereas the structure of **L^1Na** is characterized as zwitterionic form. Zwitterionic form has also been proven by single-crystal X-ray diffraction for **L^1Na**. UV–vis and NMR spectroscopies for the monosodium salts are in agreement with FT-IR results. According to these methods, all the monosodium salts have the phenol-imine form in solution.

The analytical and physical data are compatible with the proposed structures for iron(III) complexes. Elemental analyses suggest the complexes have a 1 : 2 stoichiometry, six-coordinate with the [*N*-(5-nitro-salicylidene)-D-amino acid] ligand. Magnetic susceptibility measurements show that the complexes are high-spin and paramagnetic at room temperature. From conductivity studies, they are 1 : 1 electrolytes. In the XPS spectrum, the binding energy of $Fe2p_{1/2}$ peak has been observed between 723 and 724 eV, although the binding energy of $Fe2p_{3/2}$ peak is 710 eV.

The monosodium salts have been evaluated for their antioxidant activity. The results show that **L^1Na** and **L^2Na** are moderately active in methanolic and aqueous solutions. **L^3Na** shows moderate active in methanolic solution and is more active than ascorbic acid in aqueous solution.

Supplementary material

CCDC 1003423 contains the supplementary crystallographic data for the complex. These data can be obtained free of charge via http://www.ccdc.cam.ac.uk/data_request/cif (or from the Cambridge Crystallographic Data Center, 12 Union Road, Cambridge CB2 1EZ, UK; Fax: +44-1223-336-033; E-mail: deposit@ccdc.cam.ac.uk or www: http://www.ccdc.cam.ac.uk).

Acknowledgements

We are grateful to Research Foundation of Gazi University for supporting this study with the project F.E.F.05/2011-24. We are also thankful to Aksaray University Science and

Technology Application and Research Center for the use of the Bruker SMART BREEZE CCD diffractometer (purchased under grant number 2010K120480 of the State of Planning Organization).

Disclosure statement

No potential conflict of interest was reported by the authors.

References

[1] C. Hu, W. Zhang, Y. Xu, H. Zhu, X. Ren, C. Lu, Q. Meng, H. Wang. *Transition Met. Chem.*, **26**, 700 (2001).
[2] M. Wang, Z. Meng. *Appl. Radiat. Isot.*, **64**, 235 (2006).
[3] A.M. Asiri, S.A. Khan, H.M. Marwani, K. Sharma. *J. Photochem. Photobiol., B*, **120**, 82 (2013).
[4] H. Keypour, A.H. Jamshidi, M. Rezaeivala, L. Valencia. *Polyhedron*, **52**, 872 (2013).
[5] E. Gungor, S. Celen, D. Azaz, H. Kara. *Spectrochim. Acta, Part A*, **94**, 216 (2012).
[6] R. Ramesh, S. Maheswaran. *J. Inorg. Biochem.*, **96**, 457 (2003).
[7] K.S. Kumar, S. Ganguly, R. Veerasamy, E. De Clercq. *Eur. J. Med. Chem.*, **45**, 5474 (2010).
[8] A. Das, M.D. Trousdale, S. Ren, E.J. Lien. *Antiviral Res.*, **44**, 201 (1999).
[9] S.M. Sondhi, N. Singh, A. Kumar, O. Lozach, L. Meijer. *Bioorg. Med. Chem.*, **14**, 3758 (2006).
[10] S.M. Sondhi, S. Rajvanshi, M. Johar, N. Bharti, A. Azam, A.K. Singh. *Eur. J. Med. Chem.*, **37**, 835 (2002).
[11] K.V. Sujith, J.N. Rao, P. Shetty, B. Kalluraya. *Eur. J. Med. Chem.*, **44**, 3697 (2009).
[12] M.S. Alam, J.H. Choi, D.U. Lee. *Bioorg. Med. Chem.*, **20**, 4103 (2012).
[13] S.M. Pradeepa, H.S. Bhojya Naik. *Spectrochim. Acta, Part A*, **115**, 12 (2013).
[14] K. Konarikova, L. Andrezalova, P. Rapta, M. Slovakova, Z. Durackova, L. Laubertova, H. Gbelcova, L. Danisovic, D. Bohmer, T. Ruml, M. Sveda, I. Zitnanova. *Eur. J. Pharmacol.*, **721**, 178 (2013).
[15] M.B. Gholivand, F. Ahmadi, E. Rafiee. *Electroanalysis*, **18**, 1620 (2006).
[16] S. Gago, J.E. Rodríguez-Borges, C. Teixeira, A.M. Santos, J. Zhao, M. Pillinger, C.D. Nunes, Z. Petrovski, T.M. Santos, F.E. Kühn, C.C. Romão, I.S. Gonçalves. *J. Mol. Catal. A: Chem.*, **236**, 1 (2005).
[17] H. Liu, H.-L. Zhang, S.-J. Wang, A.-Q. Mi, Y.-Z. Jiang, L.-Z. Gong. *Tetrahedron: Asymmetry*, **16**, 2901 (2005).
[18] S. Vijayalakshmi, S. Kalyanaraman. *Opt. Mater.*, **35**, 440 (2013).
[19] H.C. Sampath Kumar, B. Ramachandra Bhat, B.J. Rudresha, R. Ravindra, R. Philip. *Chem. Phys. Lett.*, **494**, 95 (2010).
[20] G. Ceyhan, M. Tümer, M. Köse, V. McKee, S. Akar. *J. Lumin.*, **132**, 2917 (2012).
[21] S. Samshuddin, B. Narayana, B.K. Sarojini, M.T.H. Khan, H.S. Yathirajan, C.G.D. Raj, R. Raghavendra. *Med. Chem. Res.*, **21**, 2012 (2012).
[22] S. Samshuddin, B. Narayana, B.K. Sarojini, L.N. Madhu. *Med. Chem. Res.*, **22**, 3002 (2013).
[23] N.A. Shakil, M.K. Singh, M. Sathiyendiran, J. Kumar, J.C. Padaria. *Eur. J. Med. Chem.*, **59**, 120 (2013).
[24] S. Milardović, D. Iveković, B.S. Grabarić. *Bioelectrochemistry*, **68**, 175 (2006).
[25] G.M. Sheldrick. *Acta Crystallogr.*, **64**, 112 (2008).
[26] *Bruker APEX2, SAINT and SADABS*. Bruker AXS Inc., Madison, WI (2012).
[27] L.J. Farrugia. *J. Appl. Crystallogr.*, **45**, 849 (2012).
[28] O.V. Dolomanov, L.J. Bourhis, J.A.K. Gildea, H. Puschmann. *J. Appl. Crystallogr.*, **42**, 339 (2009).
[29] O.P. Sharma, T.K. Bhat. *Food Chem.*, **113**, 1202 (2009).
[30] A.L. Dawidowicz, D. Wianowska, M. Olszowy. *Food Chem.*, **131**, 1037 (2012).
[31] J.C. Zhuo. *Magn. Reson. Chem.*, **37**, 259 (1999).
[32] Ö. Güngör, P. Gürkan. *Spectrochim. Acta, Part A*, **77**, 304 (2010).
[33] H. Pizzala, M. Carles, W.E.E. Stone, A. Thevand. *J. Chem. Soc., Perkin Trans.*, **2**, 935 (2000).
[34] P.M. Dominiak, E. Grech, G. Barr, S. Teat, P. Mallinson, K. Woźniak. *Chem. Eur. J.*, **9**, 963 (2003).
[35] Y. Elerman, M. Kabak, A. Elmali, I. Svoboda. *Acta Crystallogr. C*, **54**, 128 (1998).
[36] M. Yıldız, H. Ünver, D. Erdener, N. Ocak, A. Erdönmez, T. Nuri Durlu. *Cryst. Res. Technol.*, **41**, 600 (2006).
[37] L.H. Abdel-Rahman, R.M. El-Khatib, L.A.E. Nassr, A.M. Abu-Dief. *Arabian J. Chem.*, (2013), Article in press. doi:10.1016/j.arabjc.2014.01.013.
[38] L.H. Abdel-Rahman, R.M. El-Khatib, L.A.E. Nassr, A.M. Abu-Dief, F. El-Din Lashin. *Spectrochim. Acta, Part A*, **111**, 266 (2013).
[39] Y.H. Fan, X.T. He, C.F. Bi, F. Guo, Y. Bao, R. Chen. *Russ. J. Coord. Chem.*, **33**, 535 (2007).
[40] E. Canpolat, A. Yazıcı, M. Kaya. *J. Coord. Chem.*, **60**, 473 (2007).
[41] M. Rapta, P. Kamaras, G.B. Jameson. *Polyhedron*, **15**, 1943 (1996).

[42] W.J. Geary. *Coord. Chem. Rev.*, **7**, 81 (1971).
[43] Ö. Güngör, P. Gürkan. *J. Mol. Struct.*, **1074**, 62 (2014).
[44] J.L. Hueso, J.P. Espinós, A. Caballero, J. Cotrino, A.R. González-Elipe. *Carbon*, **45**, 89 (2007).
[45] D. Uzun, H. Arslan, A. Balaban Gündüzalp, E. Hasdemir. *Surf. Coat. Technol.*, **239**, 108 (2014).
[46] H. Ekşi, V.K. Gupta, Z. Üstündağ, N. Atar, M.O. Cağlayan, A.O. Solak. *J. Mol. Liq.*, **187**, 49 (2013).
[47] O. Ivashenko, J.T. van Herpt, B.L. Feringa, W.R. Browne, P. Rudolf. *Chem. Phys. Lett.*, **559**, 76 (2013).
[48] S. Biniak, G. Szymański, J. Siedlewski, A. Świątkowski. *Carbon*, **35**, 1799 (1997).
[49] B. Wang, F. Gao, H. Ma. *J. Hazard. Mater.*, **144**, 363 (2007).
[50] Q.H. Wu, A. Thißen, W. Jaegermann. *Appl. Surf. Sci.*, **252**, 1801 (2005).
[51] T. Yamashita, P. Hayes. *Appl. Surf. Sci.*, **254**, 2441 (2008).
[52] O.P. Sharma, T.K. Bhat. *Food Chem.*, **113**, 1202 (2009).
[53] N. Vukovic, S. Sukdolak, S. Solujic, N. Niciforovic. *Food Chem.*, **120**, 1011 (2010).